XVIII International Conference on Water Resources
CMWR 2010
J. Carrera (Ed)

ADAPTIVE MULTI-LEVEL MODELLING OF COUPLED MULTISCALE PHENOMENA WITH APPLICATIONS TO METHANE EVOLUTION IN SUBSURFACE

Viviane Klein* **and Małgorzata Peszyńska†**

*†Department of Mathematics, Oregon State University Corvallis, OR, 97330, USA
e-mail: *kleinv@math.oregonstate.edu, †: mpesz@math.oregonstate.edu

Key words: Error estimates, parabolic systems, double-diffusion models, modelling methane hydrates, coal-bed methane

Summary. We develop error estimates for a system of reaction–diffusion equations which are robust in parameters and therefore are applicable to degenerate cases. We show applications to models of methane evolution with kinetic exchange terms; these include multiscale and adsorption models relevant to ECBM as well as kinetic phase transition models for evolution of methane hydrates.

1 INTRODUCTION

Adaptive finite element modelling is a well developed and popular tool for simulation of important phenomena from science and engineering. The theory underlying grid adaptation involves a-posteriori error estimates available for scalar linear equations [1, 2, 3], as well as for to non-linear and degenerate problems [4, 5].

However, theory for systems of equations is less developed since the individual component equations of a system may be of different type and their solutions may exhibit disparate regularity. At the same time, many problems in water resources are described by coupled systems of partial differential equations. In this paper we consider several applications which share a common element: a coupled parabolic reaction-diffusion system. We extend residual type estimators and theory proposed in [6] and apply them to kinetic models of adsorption, multiscale couplings, and phase transition. The key behind the applicability is the robustness of the estimates following [7] and decomposition of the errors into spatial and temporal parts as in [3, 2]; our focus here is on the former.

In the paper we use standard notation for the norms in spaces C^m, L^p, and H^k defined over an open bounded convex polygonal region $\Omega \subseteq R^d$. Our theory works for $d = 1, 2, 3$, but examples cover only $d = 1$. As for time dependence, we consider $t \in I := (0, T], T > 0$; we denote by w_τ on $[0, T]$ the interpolator of a sequence $\{w^n\}_{0 \le n \le N}$. The symbol $w^n(\cdot)$ if not otherwise defined denotes $w(\cdot, t_n)$, $t_n \in I$. On $L^2(\Omega)$ we have the usual scalar product denoted by $(\cdot, \cdot)$ and the norm $\| \cdot \|$. We also use standard finite element notation [1] and

in particular we denote by $[\partial_\nu w]_E$ the jump of the normal derivative of w across an edge E of an element.

2 MODEL, ILLUSTRATION, AND THEORETICAL RESULTS

Consider nonnegative parameters $\mathcal{P} = \{\lambda_1, \lambda_2, a, b, c\}$ and the system of equations parametrized by $\mathcal{P}$

$$\lambda_1 u_t - \nabla \cdot (a \nabla u) + c(u - v) = f, \ x \in \Omega, t \in I, \tag{1}$$
$$\lambda_2 v_t - \nabla \cdot (b \nabla v) - c(u - v) = g, \ x \in \Omega, t \in I, \tag{2}$$

with homogeneous boundary conditions on $\partial\Omega$ and initial data u_0, v_0, as well as sources f, g, smooth enough to guarantee well-posedness and regularity of weak solutions to (1)-(2) sufficient for the theory to apply [8]. In particular, if all constants in $\mathcal{P}$ are positive, standard results apply. If $b = 0, g \equiv 0$, we will refer to the system (1)-(2) as a *kinetic model*; in this case extra smoothness of data is needed for optimal convergence. Figure 1 illustrates the effect of $\mathcal{P}$ on the solutions.

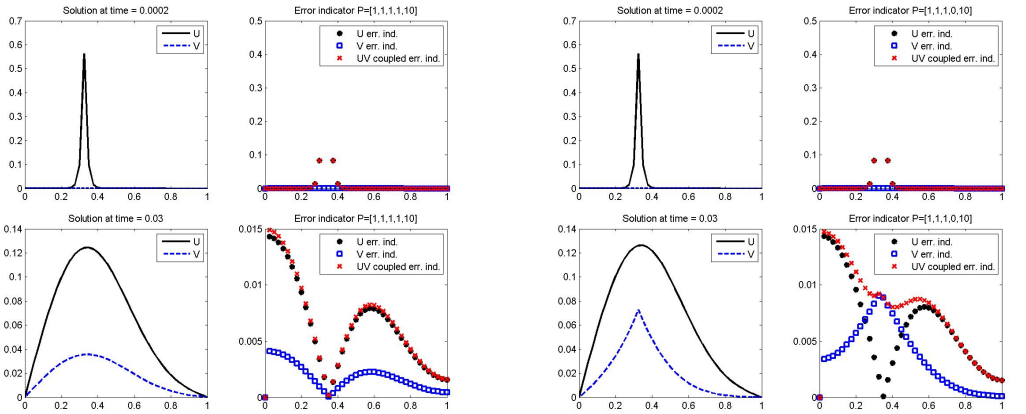

$\mathcal{P} = [1, 1, 1, 1, 10]$ $\mathcal{P} = [1, 1, 1, 0, 10]$

Figure 1: Behavior of solutions u, v to (1)–(2) and of spatial error indicators $[\partial_\nu u], [\partial_\nu v]$ for different $\mathcal{P}$. We use homogeneous initial and boundary conditions and $g \equiv 0$ and a point source at $x = 1/3$. Notice the difference in scales and in qualitative behavior of u, v for different $\mathcal{P}$. In particular, the error in v is always small at initial time steps but when $b = 0$ it may dominate the global error long after u is smooth.

Now we define the discretization of (1)-(2). For temporal discretization, we introduce a partition of I: $0 = t_0 < t_1 < \ldots < t_N = T$, and set $\tau_n := t_n - t_{n-1}$, $\Delta t = \max_n \tau_n$. For spatial discretization, we use classical Galerkin linear finite elements [1, 2, 3]. First, we define a family of admissible and shape regular partitions $\mathcal{T}_h$ over Ω, with the collection of edges $\mathcal{E}_h$. We set $h_S := diam(S), S \in \mathcal{T}_h \cup \mathcal{E}_h$ and $h := \max h_T, T \in \mathcal{T}_h$. Next, $\tilde{\omega}_T$ denotes the neighborhood of $T \in \mathcal{T}_h$, and ω_E the one of $E \in \mathcal{E}_h$. Denote by V_h the usual space of conforming piecewise linear finite elements over $\mathcal{T}_h$.

The multilevel discretization is defined via two partitions $\mathcal{T}_h, \mathcal{T}_H$ and two spaces V_h, V_H. We require that V_h be a refinement of V_H and define natural grid transfer operators: the interpolation operator $\lambda : V_H \to V_h$ and a projection operator $\lambda' : V_h \to V_H$ defined by $(\lambda'\phi_h, \psi) := (\phi_h, \lambda\psi_H), \forall \psi_H \in V_H, \phi_h \in V_h$.

Let $1 \leq n \leq N$ and define the fully discrete solution $(u_h^n, v_H^n) \in V_h \times V_H$ satisfying

$$(\frac{u_h^n - u_h^{n-1}}{\tau_n}, \phi_h) + (a\nabla u_h^n, \nabla\phi_h) + (c(u_h^n - \lambda v_H^n), \phi_h) = (f^n, \phi_h), \forall \phi_h \in V_h \quad (3)$$

$$(\frac{v_H^n - v_H^{n-1}}{\tau_n}, \psi_H) + (b\nabla v_H^n, \nabla\psi_H) + (c(v_H^n - \lambda' u_h^n), \psi_H) = (g^n, \psi_H), \forall \psi_H \in V_H \quad (4)$$

A-priori estimates will be discussed elsewhere; see Table 1 for convergence results.

2.1 A-posteriori error estimates

Here we state the estimates for $h = H$; the general case and proofs will be given elsewhere. We are interested in the error $[[(u - u_{h\tau}, v - v_{h\tau})]](t_n)$ where the energy norm is

$$[[(u,v)]]^2(t) := \left(\|u(t)\|^2 + \|v(t)\|^2 + \int_0^t \left(\|a^{1/2}\nabla u\|^2 + \|b^{1/2}\nabla v\|^2 + \|c^{1/2}(u-v)\|^2 \right) ds \right). \quad (5)$$

The error can be formally divided into spatial, temporal, and data components [3, 2]; here we are mainly interested in the former and in the robustness in $\mathcal{P}$. The *temporal error indicator* is

$$\eta_n := \sqrt{\frac{\tau_n}{3}} \left(\|a^{1/2}\nabla(u_h^n - u_h^{n-1})\| + \|b^{1/2}\nabla(v_H^n - v_H^{n-1})\| + \|c^{1/2}((u_h^n - v_h^n) - (u_h^{n-1} - v_H^{n-1}))\| \right),$$

and the *spatial error indicator*

$$\eta_{n,T} := \left(\theta_{u,T}^2 \|R_{T,u}^n\|_T^2 + \theta_{v,T}^2 \|R_{T,v}^n\|_T^2 + \frac{1}{2} \sum_{e \in \mathcal{E}_T} \left(\gamma_{u,e}^2 \|R_{e,u}^n\|_e^2 + \gamma_{v,e}^2 \|R_{e,v}^n\|_e^2 \right) \right) \quad (6)$$

where the various element and edge terms are $R_{T,u}^n := f^n - \frac{u_h^n - u_h^{n-1}}{\tau_n} + \nabla\cdot(a\nabla u_h^n) - c(u_h^n - v_h^n)$, $R_{T,v}^n := g^n - \frac{v_h^n - v_h^{n-1}}{\tau_n} + \nabla\cdot(b\nabla v_h^n) - c(v_h^n - u_h^n)$, $R_{e,u}^n := [a\partial_\nu u_h^n]_e$, $R_{e,v}^n := [b\partial_\nu v_h^n]_e$. The scaling factors are as proposed for scalar problems in [6] following [7]

$$\theta_{u,S} := \min\{h_S a^{-1/2}, \max\{c^{-1/2}, h_S b^{-1/2}\}\}, \ S \in \mathcal{T}_h \cup \mathcal{E}_h, \quad (7)$$

$$\theta_{v,S} := \min\{h_S b^{-1/2}, \max\{c^{-1/2}, h_S a^{-1/2}\}\}, \ S \in \mathcal{T}_h \cup \mathcal{E}_h, \quad (8)$$

$$\gamma_{u,e} := 2h_e^{-1/2}\theta_{u,e}, \ \gamma_{v,e} := 2h_e^{-1/2}\theta_{v,e}. \quad (9)$$

The following upper bound can be proven using techniques from [3, 2] with extension to multilevel discretizations similarly to [6]. At this time, we do not have a lower bound result of the type that we proved for the stationary case in [6].

Table 1: Error (top) and estimator (middle) and efficiency index (bottom) for $\mathcal{P} = \{1, 1, 1, b \downarrow 0, 1\}$. First order convergence is evident for the error and estimator. Efficiency index remains bounded as $b \downarrow 0$ i.e. the estimator is robust in b. Moreover, the case $b = 0$ appears as a limit of $b \downarrow 0$. The estimator is also robust in other parameters in $\mathcal{P}$ (not shown).

N_{el}/ b	1	10^{-2}	10^{-4}	10^{-6}	0
100	0.0010838	0.0010805	0.0010805	0.0010805	0.0010805
200	0.00048358	0.00048163	0.00048161	0.00048161	0.00048161
400	0.00022791	0.00022698	0.00022697	0.00022697	0.00022697
800	0.00011005	0.00010973	0.00010972	0.00010972	0.00010972

N_{el}/ b	1	10^{-2}	10^{-4}	10^{-6}	0
100	0.0069226	0.0069156	0.0069156	0.0068876	0.0068873
200	0.0034615	0.0034580	0.0034580	0.0034444	0.0034438
400	0.0017308	0.0017290	0.0017290	0.0017231	0.0017219
800	0.00086538	0.00086451	0.00086450	0.00086323	0.00086097

N_{el}/ b	1	10^{-2}	10^{-4}	10^{-6}	0
100	6.3875	6.4003	6.4004	6.3746	6.3743
200	7.1580	7.1798	7.1800	7.1518	7.1507
400	7.5939	7.6174	7.6176	7.5915	7.5865
800	7.8634	7.8789	7.8789	7.8673	7.8467

Theorem 1 *Assume u, v solve* (1)-(2) *and that the numerical solution is defined as in* (3)-(4). *Then the following upper bound for the a-posteriori error estimator holds for all* $1 \leq n \leq N$

$$[[u-u_{h\tau}]](t_n) \leq C \left(\sum_{m=1}^{n} \left(\eta_m^2 + \tau_m \sum_{T \in \mathcal{T}_{m,h}} \eta_{m,T}^2 \right) \right)^{1/2} + \text{higher order terms}(u_0, v_0, f, g).$$

The estimator $\eta_{n,T}$ is robust in the coefficients that is, its efficiency index remains bounded when, in particular, $b \downarrow 0$, When $b = 0$, an analogous result to Theorem 1 holds with the modified energy norm and estimator. For norm, we use (5) in which we set $b = 0$. For the new estimator $\eta^0_{n,T}$, we drop the edge term $R_{e,v}$ in (6) and instead of scaling factor $\theta_{v,T}$ we use $\theta^0_{v,T} := \max\{c^{-1/2}, h_T a^{-1/2}\}$. We also define $\eta^0_{n,T} := \left(\frac{h_T^2}{a} \|R^n_{T,u}\|^2 + (\theta^0_{v,T})^2 \|R^n_{T,v}\|^2 + \frac{1}{2} \sum_{e \in \mathcal{E}_T} \frac{h_e}{a} \|R_{e,u}\|^2 \right)$.

Table 1 shows convergence and robustness results for a case with known analytical solution on $\Omega = (0, 1)$. In the next Section we discuss applications where such an estimator can guide simultaneously the multilevel grid adaptivity and model selection.

3 APPLICATIONS

Models of preferential flow or diffusion of contaminants in heterogeneous reservoirs take the form of scalar elliptic or parabolic equations similar to (1) with $c = 0$, with

coefficients λ_1, a that depend on x and/or u. The additional equation in (1)–(2) may account for transient multiscale effects and/or non-equilibrium effects in adsorption and phase transitions, see examples below. A separate class of models to which our theory applies are pseudo-parabolic equations and systems [9, 10].

3.1 Multiscale models, adsorption models and ECBM

In highly heterogeneous porous media such as fissured rocks where λ, a vary strongly with x, various models help to account for associated nonlocal temporal effects, see *double-porosity models* [11, 12, 13]. Earlier models include the *double–diffusion model* [14] of the form identical to (1)–(2) where $\mathcal{P} = \{small, large, large, small, c\}$ reflects the high diffusivity of the "fast medium" and the preferential storage characteristics of the "slow medium". Its special case i.e. the Warren-Root model [15] uses $b = 0$ i.e. $\mathcal{P} = \{small, large, large, 0, c\}$. Our numerical model and estimates apply directly to this family of models; an illustration was provided in Figure 1 and Table 1. The robustness of the estimates allows to compare models with different b while maintaining a desired level of numerical error.

Next we discuss the model of diffusion and adsorption in porous reservoir Ω of porosity ϕ given by $\phi u_t + (1-\phi)v_t - \nabla \cdot (a\nabla u) = 0$, with $v = F_I(u)$ in equilibrium where F_I denotes the equilibrium isotherm [16]. A non-equilibrium coupled model reads

$$(1-\phi)v_t + c(v - F_I(u)) \;=\; 0, \tag{10}$$

where c is the *relaxation time*. Our estimates apply to this system when the isotherm is linear because then we have (1)–(2) with $\mathcal{P} = \{\frac{\phi}{1-\phi}, 1, \frac{a}{1-\phi}, 0, c\}$. Extension to the semilinear case is under way.

Finally, we consider the Enhanced Coal-Bed Methane Recovery model [17] in which the kinetic model comes from either an adsorption- or a multiscale-type [15] approach. Ignore for simplicity the capillary pressure, gravity, and compressibility. Then the structure of the wet-gas model in coal seams and cleats i.e. two-phase immiscible flow [17] after phase summation gives an elliptic pressure equation with a kinetic exchange term coupled to the kinetic model i.e. similar to (1)–(2) with $\mathcal{P} = \{0, 1, a^*, 0, c\}$. Here the mobility a^* depends on other unknowns of the model but is bounded from below. Additionally there is a coupled gas transport model solved for gas saturation S in which a separate front may develop. Error estimates are needed to control the error in P and in saturations; our estimates only apply to the linearized version of the former.

Another example of a system with where (1)–(2) is a subsystem only, is provided by evolution of methane hydrates.

3.2 Evolution of methane hydrates

Methane hydrates are an ice-like substance abundant in sub-sea sediments. They are stable only at high pressures and low temperatures; their dynamics and formation at very

long time scales is of interest to scientists studying climate change; at short time scales it is relevant for various drilling projects.

Consider a simplified form derived from [18, 19]. We solve the nonlinear mass conservation equations for salt $N_S := (1 - S_h)\rho_l X_{lS}$, and methane concentrations $N_M := (1 - S_h)\rho_l X_{lM} + S_h\rho_h$

$$\frac{\partial}{\partial t}(\phi N_S) - \nabla \cdot (\phi(1 - S_h)D_S \nabla X_{lS}) = 0, \tag{11}$$

$$\frac{\partial}{\partial t}(\phi N_M) - \nabla \cdot (\phi(1 - S_h)D_M \nabla X_{lM}) = q_M. \tag{12}$$

The model is only considered in the region where no free gas can exist i.e. methane is dissolved in water with mass fraction $X_{lM} \leq X_{lM}^{max}$. It may also form the hydrate phase whose volume fraction is denoted by $S_h \geq 0$. Further, $X_{lM}^{max}(P, T, X_{lS})$ is the maximum solubility of methane. Here we assume that the pressure P and the temperature T follow the hydrostatic and hydrothermal equilibrium, respectively; see [20, 18] for a general case. Next, X_{lS} is the salinity, and ρ_l, ρ_s, ρ_h are appropriate density factors, and D_S, D_M are diffusivities of salt and methane in liquid phase.

The thermodynamic equilibrium is represented by

$$(X_{lM}, S_h) \in \mathbf{F} := [0, X_{lM}^{max}) \times \{0\} \cup \{X_{lM}^{max}) \times (0, 1). \tag{13}$$

Formally, one can think of (13) as an analogue to adsorption isotherm. However, since $\mathbf{F}$ has segments perpendicular to the coordinate axis, we cannot write X_{lM} as a function of S_h or vice-versa. On the other hand, we can consider a regularization of $\mathbf{F}$ via a well-defined monotone Lipschitz curve $X_{lM} = H_\epsilon(S_h)$ approximating $\mathbf{F}$ as $\epsilon \to 0$. Furthermore, we can consider a kinetic model for mass transfer in which (13) is replaced by

$$\frac{\partial}{\partial t} S_h - c(X_{lM} - H_\epsilon(S_h)) = 0. \tag{14}$$

An illustration is given in Figure 2. We note that our estimates apply to the linearized version of (12)–(14) but not to the entire coupled system including (11); analysis is forthcoming.

4 CONCLUSIONS

We have presented error estimators for finite element solution of a coupled system of self-adjoint parabolic equations where some coefficients are allowed to degenerate. Our a-posteriori estimators for such systems are robust i.e. they do not deteriorate when coefficients change by orders of magnitude. We have also discussed several applications; our estimates apply to some of them directly or indirectly. More analysis and applications are under development. Some of this work can be extended to problems with moderate advection.

This research was partially supported from NSF grant 0511190 and DOE grant 98089; Peszyńska was also partially supported as the Fulbright Research Scholar 2009-2010.

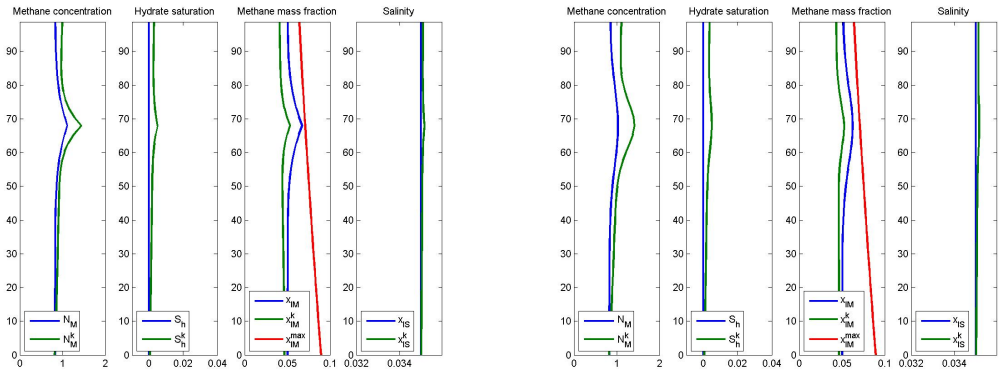

Figure 2: Solutions to the hydrate evolution models in $\Omega = (0, 100[m])$. Distance from the bottom of reservoir x is shown on vertical axis. We use N_{el}=40, and a very small Δt to accommodate stiffness of the system. Originally the system is undersaturated $X_{lM} = 0.9X_{lM}^{max}$ with salinity at seawater values $X_{lS} = 0.035$; it is subject to methane source at $x = 66[m]$ until $t = .2$ (nondimensional, left) which causes hydrate formation and small increase in salinity. This is followed by hydrate dissociation until $t = .5$ (right). Plotted values correspond to the equilibrium model (13) and kinetic (14); the latter are denoted by superscript^k. Note that the kinetic model satisfies the phase constraint only approximately while in the equilibrium model $S_h > 0$ only when $X_{lM} = X_{lM}^{max}$.

REFERENCES

[1] R. Verfürth. *A review of a posteriori error estimation and adaptive mesh-refinement techniques*. Wiley-Teubner, Chichester, 1996.

[2] R. Verfürth. A posteriori error estimates for finite element discretizations of the heat equation. *Calcolo*, 40(3):195–212, 2003.

[3] A. Bergam, C. Bernardi, and Z. Mghazli. A posteriori analysis of the finite element discretization of some parabolic equations. *Math. Comp.*, 74(251):1117–1138 (electronic), 2005.

[4] R. Verfürth. A posteriori error estimates for nonlinear problems: $Lp^*r(0,T;Wp^*1,\rho(\Omega))$-error estimates for finite element discretizations of parabolic equations. *Numer. Methods Partial Differential Equations*, 14(4):487–518, 1998.

[5] R. H. Nochetto, M. Paolini, and C. Verdi. Towards a unified approach for the adaptive solution of evolution phase changes. In *Variational and free boundary problems*, volume 53 of *IMA Vol. Math. Appl.*, pages 171–193. Springer, New York, 1993.

[6] V. Klein and M. Peszyńska. Robust a-posteriori estimates for elliptic-parabolic systems. *International Journal of Numerical Analysis and Modeling*, (to appear), 2011.

[7] R. Verfürth. Robust a posteriori error estimators for a singularly perturbed reaction-diffusion equation. *Numer. Math.*, 78(3):479–493, 1998.

[8] R. E. Showalter. *Hilbert space methods for partial differential equations*. Electronic Monographs in Differential Equations, San Marcos, TX, 1994. Electronic reprint of the 1977 original.

[9] M. Peszyńska and S.-Y. Yi. Numerical methods for unsaturated flow with dynamic capillary pressure in heterogeneous porous media. *Intl. J. Numer. Anal. Modeling*, 5 Supp.:126–149, 2008.

[10] M. Peszynska, R.E. Showalter, and S.-Y.Yi. Homogenization of a pseudoparabolic system. *Applicable Analysis*, 88(9):1265–1282, 2009.

[11] T. Arbogast. The existence of weak solutions to single porosity and simple dual-porosity models of two-phase incompressible flow. *Nonlinear Analysis, Theory, Methods and Applications*, 19:1009–1031, 1992.

[12] Ulrich Hornung and Ralph E. Showalter. Diffusion models for fractured media. *J. Math. Anal. Appl.*, 147(1):69–80, 1990.

[13] M. Peszyńska and R. E. Showalter. Multiscale elliptic-parabolic systems for flow and transport. *Electron. J. Diff. Equations*, 2007:No. 147, 30 pp. (electronic), 2007.

[14] G. I. Barenblatt, I. P. Zheltov, and I. N. Kochina. Basic concepts in the theory of seepage of homogeneous liquids in fissured rocks (strata). *J. Appl. Math. Mech.*, 24:1286–1303, 1960.

[15] J. E. Warren and P. J. Root. The behavior of naturally fractured reservoirs. *Soc. Petro. Eng. Jour.*, 3:245–255, 1963.

[16] D. M. Ruthven. *Principles of adsorption and adsorption processes*. Wiley, 1984.

[17] J.-Q. Shi, S. Mazumder, K.-H. Wolf, and S. Durucan. Competitive methane desorption by supercritical co_2 injection in coal. *TiPM*, 75:35–54, 2008.

[18] M. Peszyńska, M. Torres, and A. Tréhu. Adaptive modeling of methane hydrates. In *ICCS 2010 Proceedings*. to appear.

[19] M.E. Torres, K. Wallmann, A.M. Trehu, G. Bohrmann, W.S. Borowski, and H. Tomaru. Gas hydrate growth, methane transport, and chloride enrichment at the southern summit of Hydrate Ridge, Cascadia margin off Oregon. *Earth and Planetary Science Letters*, 226(1-2):225 – 241, 2004.

[20] X. Liu and P. B. Flemings. Dynamic multiphase flow model of hydrate formation in marine sediments. *Journal of Geophysical Research*, 112:B03101, 2008.